Eur. Phys. J. B **60**, 477–481 (2007)
DOI: 10.1140/epjb/e2008-00006-4

THE EUROPEAN PHYSICAL JOURNAL B

A first principles study of cubic IrO_2 polymorph

E. Deligoz[1,a], K. Colakoglu[2], and Y.O. Ciftci[2]

[1] Aksaray University, Department of Physics, 68100, Aksaray, Turkey
[2] Gazi University, Department Of Physics, Teknikokullar, 06500, Ankara, Turkey

Received 7 March 2007 / Received in final form 15 September 2007
Published online 16 January 2008

Abstract. We have studied structural, thermodynamic, elastic, and electronic properties of cubic IrO_2 polymorph via *ab initio* calculations within the LDA and GGA approximations. Basic physical properties, such as lattice constant, bulk modulus, second-order elastic constants (C_{ij}), and the electronic band structures are calculated, and compared with available experimental values. We have, also, predicted the Young's modulus, Poison's ratio (ν), Anisotropy factor (A), sound velocities, and Debye temperature.

PACS. 62.20.-x Mechanical properties of solids – 62.20.Dc Elasticity, elastic constants – 71.22.+i Electronic structure of liquid metals and semiconductors and their alloys

1 Introduction

Due to availability of high-pressure experimental devices, such as diamond anvil cells, high-pressure polymorphs have become an attractive research area, especially in solid state physics, chemistry, and geophysics. Meanwhile there has been considerable interest in the high pressure behaviour of metal dioxides, such as IrO_2 due to their attractive electrical, optical, and electrochemical properties. IrO_2 crystallizes in the tetragonal rutile structure in ambient conditions, and its low pressure polymorphs are extensively used for electrochromic displays [1], pH sensors [2], electrode materials in advanced memory technologies [3], and high rate-high charge capacitors [4] other application areas are given by Chen et al. in a recent review article [5] and references therein.

The first theoretical study of the rutile phase of IrO_2 was performed by Matthesis [6] in a non-self consistent calculation using the linear combination of atomic orbitals method to fit augmented–plane waves (APW_LCAO). Xu et al. [7] investigated the electronic and optical properties of the same compound using self-consistent calculations based on the linear muffin tin orbitals (LMTO) method and atomic sphere approximation (ASA). More recently, de Almeida and Ahuja [8] studied the electronic and optical properties of RuO_2 and IrO_2 in rutile structure using the full-potential linearized augmented plane wave method. Tse et al. [9] studied the elastic properties of RuO_2 in three different phases (rutile, fluorite, pyrite-type) using *ab initio* methods implemented in Wien2k and Vasp.

Ono et al. [10] have recently synthesized and analyzed the pyrite-type-structured phase of IrO_2 with Pa-3 space group symmetry at high-pressure, using a laser-heated diamond anvil cell and synchrotron X-ray diffraction. The primary difference between the fluorite- and pyrite-type structures is the different positions of the oxygen atoms in each structure. In the case of the fluorite-type structure, the oxygen atoms are located at $u = 0 : 25$ in the 8c Wyckoff position with space group Fm-3m, while in the case of the pyrite-type structure, the oxygen atoms are situated at $u = 0 : 34$ in the 8c Wyckoff position with space group Pa-3 [11].

Although a few theoretical studies exist on the rutile structure (D_{4h}) of IrO_2, to the best of our knowledge, there is no other theoretical study on the pyrite-type phase of IrO_2. Therefore, the main purpose of this paper is to gain some basic theoretical information on this phase. In particular, we have focused our attention on the structural, elastic, electronic, and thermodynamical behaviours of this phase at ambient conditions and higher pressures as well. Some comparisons have been made with the results of only one experimental observation in [10] from high- pressure X-ray diffraction experiment. Also we have compared with the theoretical results of the other hard material, RuO_2 [9], with the same structure.

2 Method of calculation

The SIESTA (The Spanish Initiative for Electronic Simulations with Thousands of Atoms) code [12–14] was utilized in this study to calculate the energies and atomic forces. It solves the quantum mechanical equation for the electrons with the density functional approach in the local density approximation (LDA) parameterized by Ceperley and Alder [15] and generalized gradient approximation

[a] e-mail: edeligoz@yahoo.com

(GGA) based on Perdew et al. [16] for the electronic exchange and correlation potential. The interactions between electrons and core ions are simulated with separable Troullier–Martins [17] norm-conserving pseudopotentials. The basis set is based on the finite range pseudoatomic orbitals (PAOs) of the Sankey-Niklewsky type [18], generalized to include multiple-zeta decays. We have generated atomic pseudopotentials separately for both atoms, Ir and O by using the $6s^2 6p^0 5d^7 5f^0$ and $2s^2 2p^4 3d^0 4f^0$ atomic configurations, respectively. The cut-off radii for the present atomic pseudopotentials are taken as s: 2.60 p: 2.40 d: 2.40 f: 2.40 au for Ir, and 1.15 au for s, p, d and f channels for O. Relativistic effects are taken into account for Ir due to its heavy mass in the pseudopotential calculations. Also, all calculations have been carried out at zero temperature, and the zero-point motion of the nuclei is not taken into account in this work.

SIESTA calculates the self-consistent potential on a grid in real space. The fineness of this grid is determined in terms of an energy cut-off E_c in analogy to the energy cut-off when the basis set involves plane waves. Here by using a double-zeta plus polarization (DZP) orbitals basis and the cut-off energies between 100 and 300 Ry with various basis sets, we found its optimal values around 200 Ry. Atoms were allowed to relax until atomic forces were less than 0.04 eV Å^{-1}. For the final computations, 196 k-points were found to be adequate for obtaining total energy with accuracy about 1 meV/atom.

3 Results and discussion

3.1 Structural and electronic properties

First, the equilibrium lattice parameter was computed by minimizing the crystal total energy calculated for different values of the lattice constant by means of Murnaghan's equation of state (eos) [19] as in Figure 1. The bulk modulus, and its pressure derivative have also been estimated, based on the same Murnaghan equation of state, and the results are given in Table 1 along with the experimental values. The calculated lattice constant (a_0) using the LDA is in excellent agreement with the experimental value [10], but the same value obtained from GGA is about 5% higher than the experimental one. The LDA generally underestimates the lattice constant while the GGA overestimates the lattice constants when compared with experiment. The present values of bulk modulus obtained from LDA and GGA are about 10% (higher) and 10% (lower) than the experimental value [6], respectively. Because the calculation of equation of state (eos) is an essential step to examine the accuracy of a theoretical calculation, the variation in volume as a function of pressure is compared with experimental values of Ono et al. [10] in Figure 2. As can be seen, the predicted eos using LDA exactly follows the experimental eos.

Although it is not our main intention here to make detailed band-structure calculations, we have predicted the band structures for cubic IrO_2 polymorph along the high symmetry directions from the calculated equilibrium lattice constant as shown in Figure 3. To see the details of the bands from Ir-5d and O-2p states, the valence bands between –22 and –4 eV in energies are not seen in Figure 3. It can be seen from Figure 3 that this structure shows a metallic character (no band gap). As we stated in the introduction band structure calculations have only been performed previously [6–8] on the rutile structure of IrO_2.

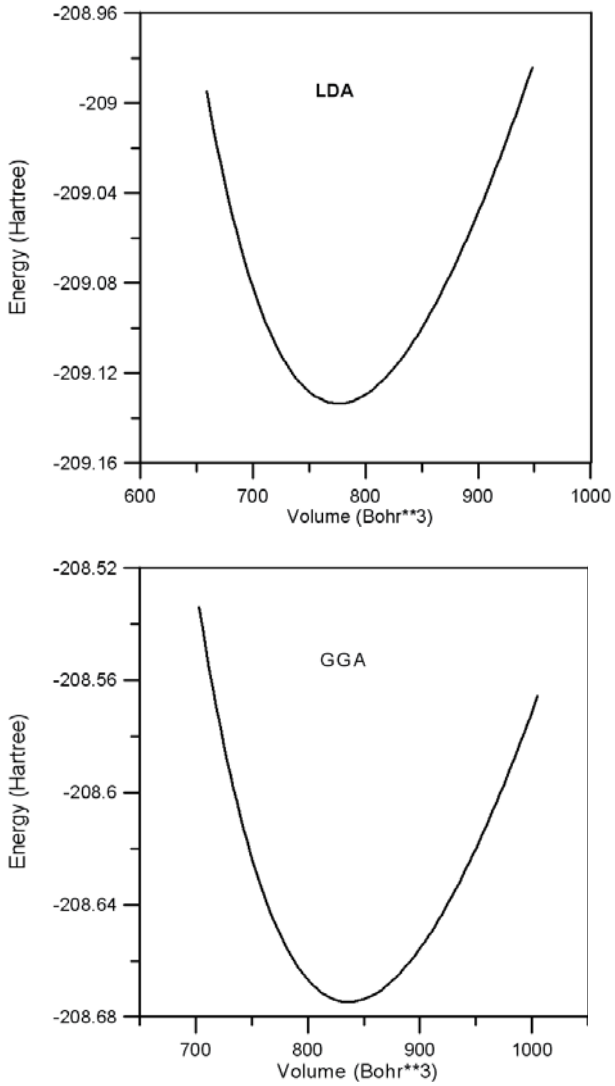

Fig. 1. Energy versus volume curves of the cubic IrO_2 polymorph.

Table 1. Calculated equilibrium lattice constant (a_0), bulk modulus (B), and the pressure derivative of bulk modulus (B'), together with the experimental value, for the cubic IrO_2 polymorph.

Material	Reference	a_0 (Å)	B (GPa)	B'
IrO_2	Present(LDA)	4.86	332.74	4.80
	Present(GGA)	4.99	269.10	5.07
	Experimental[a]	4.87	306(±6)	4.00

[a] Reference [10].

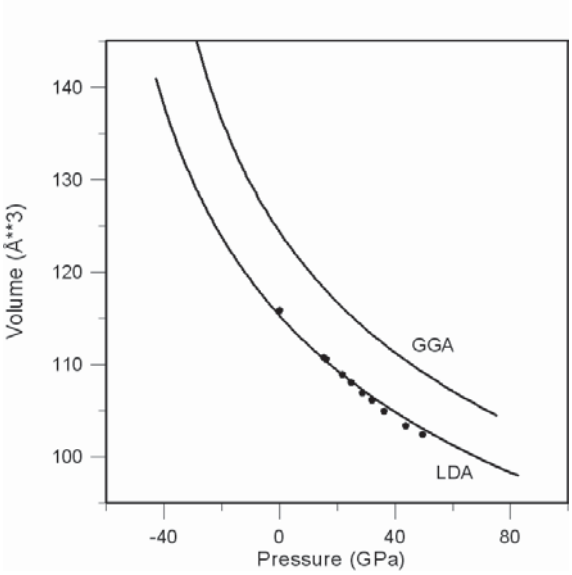

Fig. 2. Pressure versus volume curves of the cubic IrO_2 polymorph.

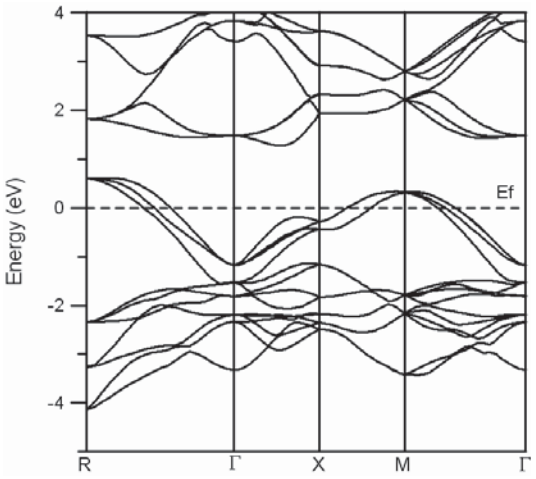

Fig. 3. Calculated band structures of the cubic IrO_2 polymorph. The position of the Fermi level is at 0 eV.

The present *ab initio* results are qualitatively similar to those of Tse et al. [9] for the pyrite-type cubic phase of RuO_2 using first principles methods.

The total and partial density of states (DOS and PDOS) corresponding to the band structures shown in Figure 3 is also indicated in Figure 4 along with the Fermi energy level. The position of the Fermi level is at 0 eV. In this figure, the lowest valence bands occur between about –22 and –20 eV and are essentially dominated by O-2*s* states, with minor presence of Ir-5*d* states. The other valence bands are essentially dominated by Ir-5*d* and O-2*p* states. The 6*s* states of Ir atoms are also contributing to the valence bands, but the values of densities of these states are quite small compared to Ir-5*d* and O-2*p*. The conduction band consists essentially of Ir-5*d* with a minor presence of O-2*p* states.

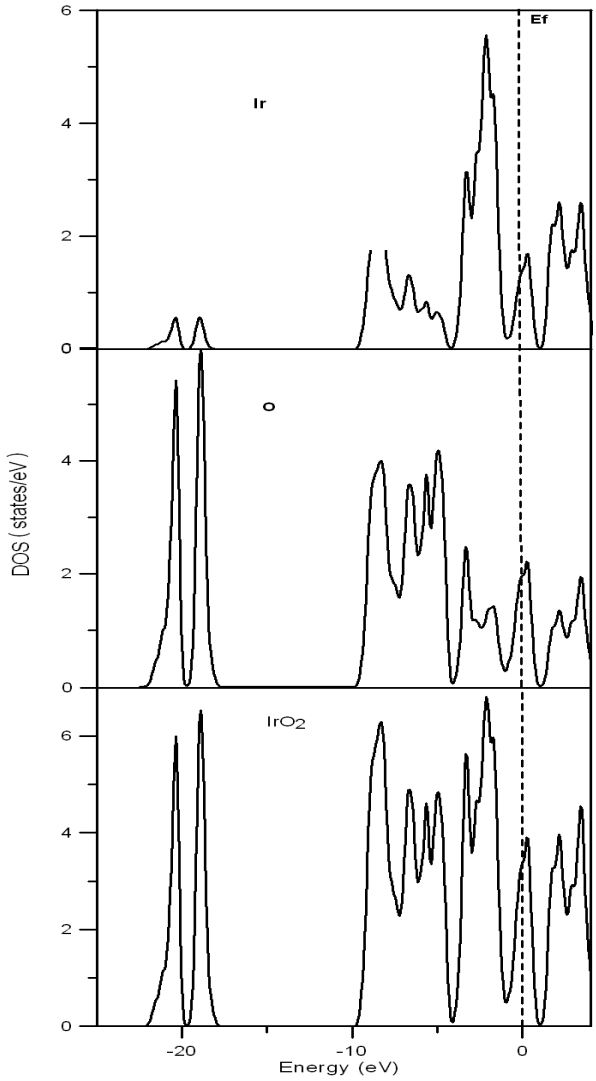

Fig. 4. The calculated total DOS and atomic projected DOS of the cubic IrO_2 polymorph. The position of the Fermi level is at 0 eV.

3.2 Elastic properties

The elastic constants of solids provide a link between the mechanical and dynamical behaviour of crystals, and give important information concerning the nature of the forces operating in solids. In particular, they provide information on the stability and stiffness of materials, and their *ab initio* calculation requires precise methods. Since the forces and the elastic constants are functions of the first-order and second-order derivatives of the potentials, their calculation will provide a further check on the accuracy of the calculation of forces in solids. The effect of pressure on the elastic constants is essential, especially for understanding interatomic interactions, mechanical stability, and phase transition mechanisms. Here for calculating the elastic constants (C_{ij}), we have used the "volume–conserving" technique [20–22] as we did recently for cadmium chalcogenides [23]. The present elastic constant values for IrO_2 are given in Table 2. It is seen from this table that the

Table 2. Elastic constants (in GPa) for the cubic IrO_2 polymorph.

Material	Reference	C_{11}	C_{12}	C_{44}
IrO_2	Present (LDA)	472.66	262.89	153.96
	Present (GGA)	384.59	211.38	133.44
	Average	428.63	237.14	143.70
RuO_2 (pyrite-type)	Theory[a]	450	189	147

[a] Reference [9].

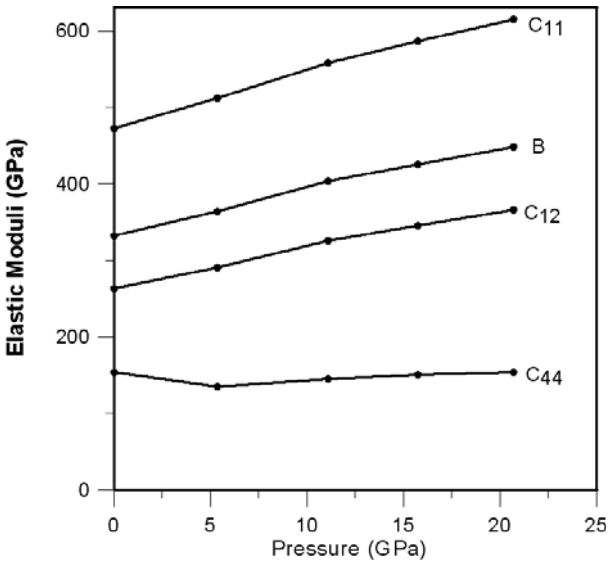

Fig. 5. The pressure dependence of C_{ij} and bulk modulus for the cubic IrO_2 polymorph.

consistency of the present results with RuO_2 is satisfactory in general except C_{12} which is higher (about 15%) than that of RuO_2.

The traditional mechanical stability conditions in cubic crystals on the elastic constants are given as $C_{11} - C_{12} > 0$, $C_{11} > 0$, $C_{44} > 0$, $C_{11} + 2C_{12} > 0$, and $C_{12} < B < C_{11}$. Our results for elastic constants in Table 2 obey these stability conditions.

We have also calculated the pressure dependency of the second-order elastic constants (SOEC) for the cubic IrO_2 polymorph as seen in Figure 5. As expected, both C_{11} and C_{12} increase monotonically with pressure whereas the slope for C_{44}, relatively, is lower. Meanwhile, the predicted pressure derivatives of elastic constants, $\frac{\partial C_{11}}{\partial P}$, $\frac{\partial C_{12}}{\partial P}$, and $\frac{\partial C_{44}}{\partial P}$ for IrO_2 in the pyrite phase are found to be 6.96, 5.03, and 0.26, respectively.

The Zener anisotropy factor A, Poisson's ratio υ, and Young's modulus Y, which are the most interesting elastic properties for applications, are also calculated in terms of the computed data using the following relations [24]:

$$A = \frac{2C_{44}}{C_{11} - C_{12}}, \tag{1}$$

$$\upsilon = \frac{1}{2}\left[\frac{(B - \frac{2}{3}G)}{(B + \frac{1}{3}G)}\right], \tag{2}$$

Table 3. The calculated Zener anisotropy factor (A), Poisson's ratio (υ), Young's modulus (Y), and shear modulus for the cubic IrO_2 polymorph.

Material	Reference	A	υ	Y (GPa)	C' (GPa)
IrO_2	Present (LDA)	1.47	0.32	349.77	129.42
	Present (GGA)	1.54	0.31	295.54	110.02
	Average	1.50	0.32	322.65	119.72

and

$$Y = \frac{9GB}{G + 3B} \tag{3}$$

where $G = (G_V + G_R)/2$ is the isotropic shear modulus, G_V is Voigt's shear modulus corresponding to the upper bound of G values, and G_R is Reuss's shear modulus corresponding to the lower bound of G values; they can be written as $G_V = (C_{11} - C_{12} + 3C_{44})/5$, and $5/G_R = 4/(C_{11} - C_{12}) + 3/C_{44}$. The calculated Zener anisotropy factor (A), Poisson's ratio (υ), Young's modulus (Y), and shear modulus ($C' = (C_{11} - C_{12+}2C_{44})/4$) for the cubic IrO_2 polymorph are given in Table 3.

The Debye temperature is known as an important fundamental parameter closely related to many physical properties such as specific heat and melting temperature. At low temperatures the vibrational excitations arise solely from acoustic vibrations. Hence, at low temperatures the Debye temperature calculated from elastic constants is the same as that determined from specific heat measurements. We have calculated the Debye temperature, θ_D, from the elastic constants data using the average sound velocity, v_m, by the following common relation given in [25]

$$\theta_D = \frac{\hbar}{k}\left[\frac{3n}{4\pi}\left(\frac{N_A\,\rho}{M}\right)\right]^{1/3} v_m \tag{4}$$

where $\hbar$ is Planck's constants, k is Boltzmann's constant, N_A is Avogadro's number, n is the number of atoms per formula unit, M is the molecular mass per formula unit, $\rho(= M/V)$ is the density, and v_m is obtained from [26]

$$v_m = \left[\frac{1}{3}\left(\frac{2}{v_t^3} + \frac{1}{v_l^3}\right)\right]^{-1/3} \tag{5}$$

where v_l and v_t, are the longitudinal and transverse elastic wave velocities, respectively, which are obtained from Navier's equation [27],

$$v_l = \sqrt{\frac{3B + 4G}{3\rho}} \tag{6}$$

and

$$v_t = \sqrt{\frac{G}{\rho}}. \tag{7}$$

The calculated longitudinal, transverse, and average elastic wave velocities for IrO_2 are given in Table 4. Debye temperature is estimated (average) to be 485 K. This value for cubic IrO_2 is higher (about 10%) than those obtained for a constituent Ir atom (430 K).

Table 4. The longitudinal, transverse, and average elastic wave velocities, together with the Debye temperature, for the cubic IrO_2 polymorph.

Material	Reference	v_l(m/s)	v_t(m/s)	v_m(m/s)	θ_D(K)
IrO_2	Present (LDA)	6272.9	3197.3	3582.6	501.70
	Present (GGA)	5911.3	3060.1	3425.5	467.88
	Average	6092.1	3128.7	3504.1	484.78

4 Summary and conclusion

In this work we report, for the first time, some theoretical results on the structural, mechanical, elastic, electronic, and thermodynamical properties for the pyrite-type phase of IrO_2 based on *ab initio* total energy calculations. Our estimated lattice constant and the bulk modulus are in agreement with room-temperature experimental values in the limit of LDA and GGA. Unfortunately, for the other properties computed in this work, there are no previous calculations for comparison, so comparison can only be made with similar compounds with the same structure. Finally, we believe that more experimental and theoretical work is required on the pyrite-type and the other high pressure phases of IrO_2 to clarify these properties in all aspects.

This work is supported by Gazi University Research-Project Unit under Project No: 05/2007-42.

References

1. W.C. Dautremont-Smith, Displays **3**, 67 (1982)
2. K. Pasztor, A. Sekiguchi, N. Shimo, N. Kitamura, H. Masuhara, Sensors Actuators B **12**, 225 (1993)
3. X. Beebe, T.L. Rose, IEEE Trans. Biomed. Eng. **35**, 494 (1988)
4. T. Nakamura, Y. Nakao, A. Kamisawa, H. Takasu, Appl. Phys. Lett. **65**, 1522 (1994)
5. R.S. Chen, A. Korotcov, Y.S. Huang, D.S. Tsai, Nanotechnology **17**, R67 (2006) and references therein
6. L.F. Matthesis, Phys. Rev. B **13**, 2433 (1976)
7. I.H. Xu, T. Jarlborg, A.J. Freeman, Phys. Rev. B **40**, 7939 (1989)
8. J.S. de Almeida, R. Ahuja, Phys. Rev. B **73**, 165102 (2006)
9. J.S. Tse, D.D. Klug, K. Uehara, Z.Q. Li, J. Haines, J.M. Léger, Phys. Rev. B **61,** 10029 (2000)
10. S. Ono, T. Kikegawa, Y. Ohishi, Physica B **363**, 140 (2005)
11. J. Muscat, V. Swamy, N.M. Harrison, Phys. Rev. B **65**, 224112 (2002)
12. `http://www.uam.es/siesta`
13. P. Ordejón, E. Artacho, J.M. Soler, Phys. Rev. B (Rapid Comm.) **53,** R10441 (1996)
14. J.M. Soler, E. Artacho, J.D. Gale, A. García, J. Junquera, P. Ordejón, D. Sánchez-Portal, J. Phys.: Condens. Matt. **14**, 2745 (2002)
15. D.M. Ceperley, M.J. Alder, Phys. Rev. Lett. **45**, 566 (1980)
16. J.P. Perdew, S. Burke, M. Ernzerhof, Phys. Rev. Lett. **77**, 3865 (1996)
17. N. Troullier, J.L. Martins, Phys. Rev. B **43**, 1993 (1991)
18. O.F. Sankey, D.J. Niklewski, Phys. Rev. B **40**, 3979 (1989)
19. F.D. Murnaghan, Proc. Natl. Acad. Sci. USA **30**, 5390 (1944)
20. J. Mehl, Phys. Rev. B **47,** 2493 (1993)
21. S.Q. Wang, H.Q. Ye, Phys. Status Solidi B **240**, 45 (2003)
22. O. Gülseren, R.E. Cohen, Phys. Rev. B **65**, 641032 (2002)
23. E. Deligoz, K. Colakoglu, Y. Ciftci Physica B **373**, 124 (2006)
24. B. Mayer, H. Anton, E. Bott, M. Methfessel, J. Sticht, P.C. Schmidt Intermetallics **11**, 23 (2003)
25. J.R. Christman, Fundamentals of Solid State Physics (John Wiley & Sons, New York, 1988)
26. O.L. Anderson, J. Phys. Chem. Solids **24**, 909 (1963)
27. E. Screiber, O.L. Anderson, N. Soga, Elastic Constants and their Measurements (McGraw-Hill, New York, 1973)